Journal of Energy Storage 110 (2025) 115317

Contents lists available at ScienceDirect

Journal of Energy Storage

journal homepage: www.elsevier.com/locate/est

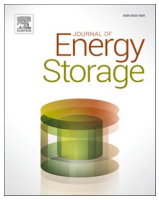

Research papers

Underground energy storage using abandoned oil & gas wells assisted by geothermal

Qitao Zhang, Arash Dahi Taleghani *, Derek Elsworth

John and Willie Leone Family Department of Energy and Mineral Engineering, Pennsylvania State University, University Park, 16801, USA

ARTICLE INFO

Keywords:
Compressed air energy storage
Abandoned oil and gas wells
Geothermal energy
Economic efficiency

ABSTRACT

The need for excessive initial investment significantly impedes the commercial development of compressed air energy storage (CAES) projects. However, the reuse of abandoned oil and gas wells (AOGWs) as containment cells for pressurized air obviates this problem and alleviates the many environmental issues caused by AOGWs. We propose a novel geothermal-assisted (GA) compressed air energy storage (GA-CAES) that integrates abundant AOGWs and ubiquitous deep geothermal heat into a single seamless CAES system. The hot reservoir rock heats the air charge within the CAES and increases system efficiency. The performance of GA-CAES using AOGWs is investigated through numerical simulations. According to the simulation results, the utilization of subsurface geothermal heat increases system efficiency. The application of AOGWs with geothermal pre-heat the air by ~160 K. Concurrently, the increase in temperature further pressurizes the air in the well by ~0.5 MPa. The input of geothermal energy increases the system round-trip efficiency by ~9.5 %. This reuse of AOGWs significantly decreases initial investment for such projects and increases system efficiency. The project payback period can be shortened by ~1 year over the usual ~3 years. The presented energy storage system can harness natural geothermal heat, thereby enhancing system efficiency and reducing initial project costs by leveraging existing infrastructure. This novel arrangement can achieve cleaner, more profitable, and more efficient CAES systems that are thus of greater viability.

1. Introduction

The success of the energy transition relies on the economic efficiency of the newly established clean energy projects. However, the large initial investment required for some classes of projects can significantly impede their further development - compressed air energy storage (CAES) is one such case in point [1]. One possible solution to increase economic efficiency is to leverage some pre-existing oil and gas infrastructure for renewable energy storage [2]. The objective of this research is to explore the feasibility of integrating abandoned oil and gas wells (AOGWs) into CAES development. The presented system can enable the leverage of the abandoned infrastructure and meanwhile address some issues from AOGWs. Such subsurface wells open the possibility to dual use of their natural geothermal heat to increase the system efficiency and decrease the initial investment of the project due to the leverage of pre-existing facilities.

Energy storage is potentially a pivotal element in the transition to clean energy. It addresses the intermittent nature of renewable sources, stabilizes the grid, and maximizes the utilization of wind and solar power. By storing excess renewable energy and releasing it when needed, energy storage contributes to grid stability and reliability [3]. Additionally, it reduces greenhouse gas emissions by displacing fossil fuel generation, promotes energy resilience in the face of extreme weather events, and supports the electrification of the transportation sector [4]. Energy storage also plays a crucial role in expanding energy access in remote areas, decentralizing the grid, and generating economic opportunities. As technology advances and costs decrease, the importance of energy storage in achieving a sustainable and clean energy future continues to grow [5]. Recently, large-scale energy storage methods like pumped hydroelectric storage (PHS) and CAES have attracted significant attention [6]. Between these two energy storage methods, CAES can provide grid-scale energy storage, providing peak power, load leveling, and ancillary services. CAES compresses air in containers for storage when the electricity demand is low, and releases it for electricity generation when the electricity demand is high. As the need for grid-scale energy storage increases, CAES and A-CAES (adiabatic compressed air energy storage) are attracting growing interest from governments, utilities, and investors [7]. Compared to PHS, CAES

* Corresponding author.
E-mail address: arash.dahi@psu.edu (A. Dahi Taleghani).

https://doi.org/10.1016/j.est.2025.115317
Received 26 August 2024; Received in revised form 2 January 2025; Accepted 3 January 2025
Available online 8 January 2025

relies less on local water resources which makes it more flexible in site selection. Besides, CAES has great potential in the integration of other kinds of energy sources like wind, solar, and geothermal energy into the grid. In the past few decades, CAES technologies have matured significantly and many CAES plants have been built since the first CAES plant in 1978. Several CAES pilot plants have been built including the Huntorf CAES plant in Germany (290 MW) [8], the Mclntosh CAES plant (110 MW) [9], and Bethel Energy Center projects (324 MW) [10] in the United States. However, most current CAES plants are diabatic, losing heat during compression with no reuse option. Meanwhile, fossil fuels are usually needed for air expansion when the air goes into the turbine train, which causes extra greenhouse gas emissions and reduces system efficiency (~50 % – 60 %) [11]. To solve this problem, A-CAES stores the heat generated during the compression cycle and reuses it before the gas expansion cycle. The system round-trip efficiency can reach 70 % or more (as in the ADELE CAES project) [12] a significant advance for CAES technology. Even though the concept of A-CAES was proposed many years ago, only a limited number of pilot A-CAES plants have been built or approved for construction - including the ADELE plant in Germany with a capacity of 20 MW. One of the key impediments to the further development of A-CAES is its higher initial investment and the need for a large volume capacity in high-pressure containers for highly efficient air storage [13]. Therefore, the utilization of abandoned oil and gas wells may help solve this problem.

Recent research has also explored the potential of repurposing abandoned mines [14] and oil reservoirs [15] as energy storage systems. These underground spaces offer unique advantages, such as stability and natural insulation, making them ideal for various energy storage technologies. One promising approach is pumped hydro storage (PHS), where water is pumped uphill to a higher reservoir during off-peak hours and released to generate electricity when demand is high. Abandoned mines can serve as natural reservoirs, eliminating the need for extensive construction [16,17]. Additionally, compressed air energy storage (CAES) is being considered, where air is compressed and stored in underground cavities during low-demand periods and released to drive turbines during peak demand [18–20]. These repurposing strategies not only address the challenges of renewable energy integration but also offer economic and environmental benefits by revitalizing abandoned sites and reducing the carbon footprint of energy production. The proposed emerging energy storage systems can also be integrated with other energy systems, such as wind and solar energy systems, to contribute to the broader energy transition [21].

As many oil and gas reservoirs in the United States are depleted, more and more oil and gas wells are being abandoned as shown in Fig. 1. Environmentally benign decommissioning is a new challenge for industry, government, and society. Currently, 130,000 “documented” orphaned wells exist in the United States (from the database of the U.S. Department of the Interior) [22] with an “estimated” 2 to 3 million abandoned wells nationwide (from the document of the U.S. Environmental Protection Agency) [23] – presenting a significant problem to address the many environmental and public health concerns. These AOGWs, or “orphan wells”, usually lack appropriate maintenance, monitoring, and even an identifiable or responsible owner. The increasing number of AOGWs presents a high risk for greenhouse gas leakage, soil contamination, underground water pollution, and the release of toxic chemicals, which significantly contribute to climate change, endanger the environment, and threaten health [24–26]. To take responsibility for addressing the significant problem of AOGWs, the U.S. government has made great efforts in recent years. For example, in 2022, The U.S. Department of the Interior awarded an initial $560 million from the Bipartisan Infrastructure Bill to 24 states to begin work to plug, cap, and reclaim orphaned oil and gas wells [27]. In addition, the Infrastructure Investment and Jobs Act (IIJA) allocated $4.75 billion to plug, remediate, and monitor orphaned wells across the U.S. [28]. Additionally, the Federal Orphaned Wells Program provides $250 million to federal land managers in the Departments of the Interior and of Agriculture to address orphaned well sites [29]. States and tribes are also implementing their own initiatives and leveraging federal funding to tackle the problem.

Despite current efforts, the increasing number of AOGWs remains a significant challenge for the government and will require billions of dollars to seal and monitor these orphan wells in the next few years. One solution to appropriately deal with such liabilities is to reuse them as assets for renewable energy and integrate them into the energy transition [2]. Here, we propose to use AOGWs as inexpensive CAES containers by sealing and converting their structure. CAES systems store

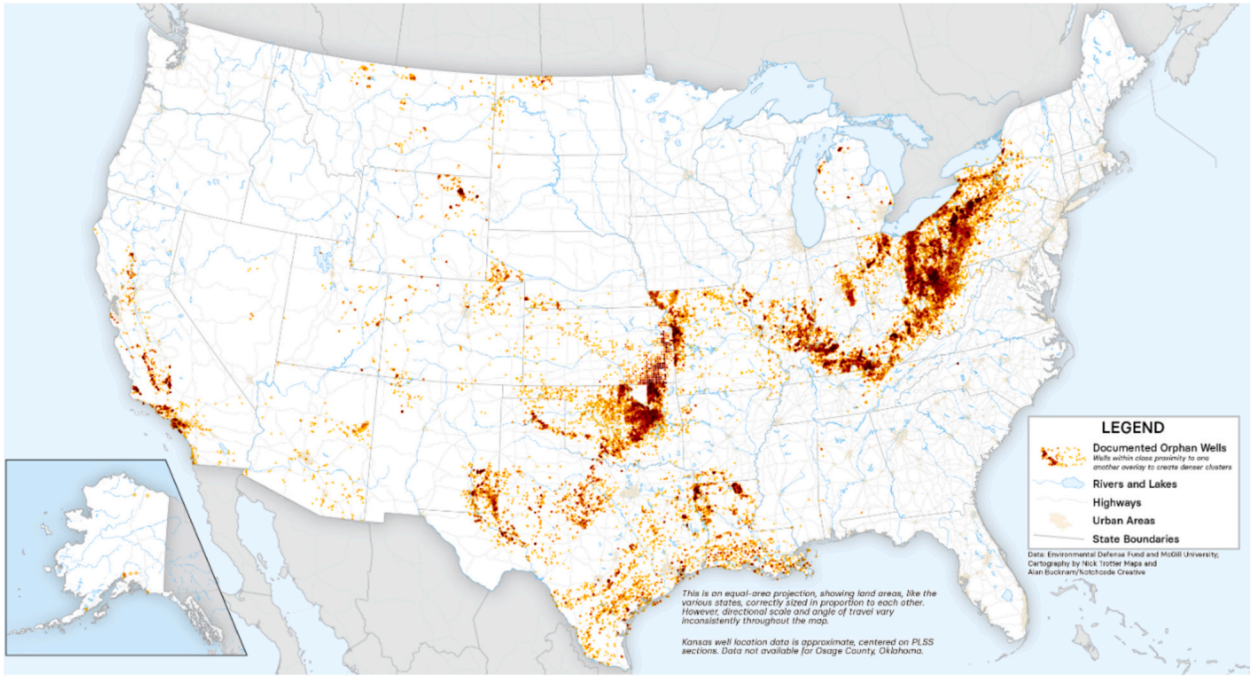

Fig. 1. Distribution of documented abandoned oil and gas wells (AOGWs) in the United States [22].

energy by compressing air and storing it in underground caverns or wells. When electricity is needed, the compressed air is released, expanding and driving a turbine and then a generator to produce electricity. We propose the use of the abandoned well itself for energy storage. Therefore, we need to seal the well at its base, beneficially staunching any release of methane into the atmosphere. Furthermore, we propose taking advantage of the underground geothermal heat to further charge (heat) the stored air by improving heat conductivity in the bottom half of the well and improving heat insulation in the top half of the wellbore. This heating from below would further increase the pressure of the stored air.

There are several other advantages to the use of abandoned wells for CAES. AOGWs typically have geological characteristics that make them favorable for CAES, such as sealed and stable rock formations. Furthermore, these wells often have existing infrastructure as wellhead valves, which can be retrofitted for CAES. Repurposing abandoned wells for CAES can also mitigate environmental risks associated with methane leakage, as well as groundwater contamination concerns [30]. However, like any innovative solution, some challenges and considerations need to be addressed before field implementation. Before repurposing an abandoned well, it is crucial to assess and ensure the integrity of the well casing and seals to prevent air or gas leakage. The repurposing of wells for CAES would need to comply with environmental regulations and the necessary permits would be required. The economic viability of such projects depends on factors such as well conditions, the availability of suitable facilities, and proximity to energy demand centers. Since our proposed design would take advantage of the natural geothermal heat, it would provide some advantages over other typical CAES systems, especially for short-term storage (a few days). Repurposing abandoned oil and gas wells for energy storage, while technically feasible, is still in the early stages in the United States. Federal funding for AOGWs may motivate such efforts, especially in communities affected by downturns in coal mining and oil and gas production. Conversely, with the increasing need for large-scale energy storage solutions to support the integration of renewable energy, it is an innovative and environmentally responsible approach to consider. Successful projects could potentially breathe new life into these wells, addressing both energy storage needs, and environmental concerns associated with the abandoned wells.

We explore the feasibility of GA-CAES (Geothermal-assisted compressed air energy storage) integrated with AOGWs. First, a conceptual model of GA-CAES is proposed (Section 2). Then, a mathematical model is used to describe the air storage in AOGWs (Section 3.1). After, the numerical model is established, and validated with reference data (Section 3.2). The results and discussions are presented in Section 3.3. In particular, we address the system round-trip efficiency where geothermal energy is naturally incorporated into the system and the increase of economic efficiency from the existing abandoned wells. Since current approaches for CAES systems demand high investment for greenfield construction, CAES systems combining AOGWs and geothermal energy offer economic advantages and may expedite the development of CAES projects.

The novelty of this research lies in its innovative approach to repurposing existing subsurface infrastructure – abandoned oil and gas wells, for energy storage applications. By integrating geothermal energy into the system, the researchers are not only increasing the overall efficiency but also reducing the environmental impacts and initial investment costs. This dual-purpose utilization of existing resources represents a significant advancement in sustainable energy solutions, offering a promising pathway towards a more resilient and environmentally friendly energy future.

2. Conceptual design of GA-CAES with AOGWs

In the following, we integrate AOGWs into the energy storage system and further increase the round-trip efficiency using geothermal heat to decrease the project payback period of the CAES system. We present our novel concept of geothermal-assisted adiabatic compressed air energy storage (GA-CAES), which can simultaneously engage multiple adjacent AOGWs in an integrated and scalable energy storage system.

The configuration of a conventional CAES is shown in Fig. 2. For a CAES project nowadays, caverns and aquifers are widely utilized as containers of compressed air [31,32]. During the charging process, the air is first pressurized in the compression train and then pumped into the air storage chambers like caverns and aquifers for storage purposes. Between each compressor, the intercooler should be installed to avoid excessive air temperature. During the discharging process, the compressed air from air storage chambers will be pulled out and heated up again through the combustion of fossil fuel. Then the high pressure and high temperature compressed air can drive the turbines to generate electricity when the electricity demand is high. Even though some CAES projects have been built up in the past few decades, conventional CAES still have problems that impede their commercial usage. One of the main problems is that conventional CAES cannot make use of the heat generated during the charging process and it still needs to burn fossil fuel during the discharging process. Another problem is that the initial investment in a conventional CAES is huge which makes it difficult for the company to profit through these projects.

In contrast, we propose a GA-CAES with the utilization of AOGWs in energy storage, which can enable operators to better manage air storage and repurpose preexisting facilities. To repurpose the AOGWs into energy storage applications, production zones at the well toe must first be sealed to prevent leakage of methane into the active wellbore and hence the environment. The application of AOGWs in CAES not only enables the utilization of pre-existing facilities in the field and decreases the initial investment for the project, but also enables the utilization of subsurface geothermal energy to pre-heat and further pressurize the air stored in the wells. By improving thermal conductivity in the bottom half of the well and improving heat insulation in the top half of the well, the hot downhole environment can pre-heat the air before entering the turbines without using the recuperator, potentially increasing the system's efficiency. Dual-layer tubing strings available commercially can provide insulation for the top part of the wellbore. Considering that the wells should be sealed before these applications, therefore the outcome of the storage will be independent of the geology.

The full configuration of the designed GA-CAES is shown in Fig. 3. Air is sequentially pressurized by a series of compressors from low pressure to high pressure. Between the compressors, intervening refrigeration heat exchangers (intercoolers, ICs) should be installed to cool down the air from the compressor with low pressure and thus prevent the overheating problem. These ICs and AC (aftercooler) can capture the heat generated during the compression process and then temporarily store it in the thermal energy storage (TES) tank. The stored heat in the TES is later reused for gas expansion to drive the train of the turbine – thus these heat exchangers and TES ensure the “adiabatic” performance on the surface (all the heat generated in air compression can be used in air expansion). Air exiting the CP4 (node 8 in Fig. 3) drops to near ambient external temperature. The compressed air is pumped into the AOGWs for energy storage and pre-heated by the hot reservoir environment. When the air leaves the AOGWs during the discharging process, we assume that the air pressure is controlled via the Joule-Thomson throttling. For GA-CAES with AOGW, we can use the pre-existing wellhead facilities as the regulator valve. Considering the narrow range of variations of the Joule-Thomoson coefficient, it is presumed that the real gas effects are neglected, and the throttling process is isothermal, i.e., the air temperature before and after traveling the valve should be the same. During the discharge stage, compressed air again flows through the TES and is reheated. Thermal energy aids air expansion and then drives the turbine train of high-pressure (HPT) and then low-pressure turbines (LPT), for electricity generation.

Fig. 4 shows the application of AOGWs in utilizing geothermal energy: (1) First, the cold and compressed air from the last compressor is pumped into wells when the electricity demand is low. (2) Then, wells

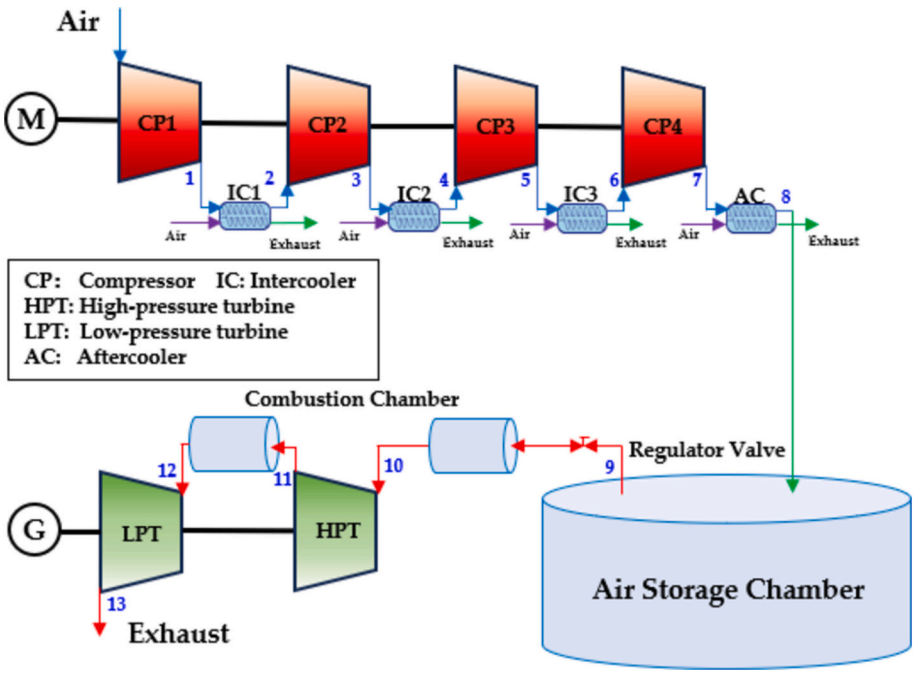

Fig. 2. Configuration of a conventional CAES with caverns or aquifers.

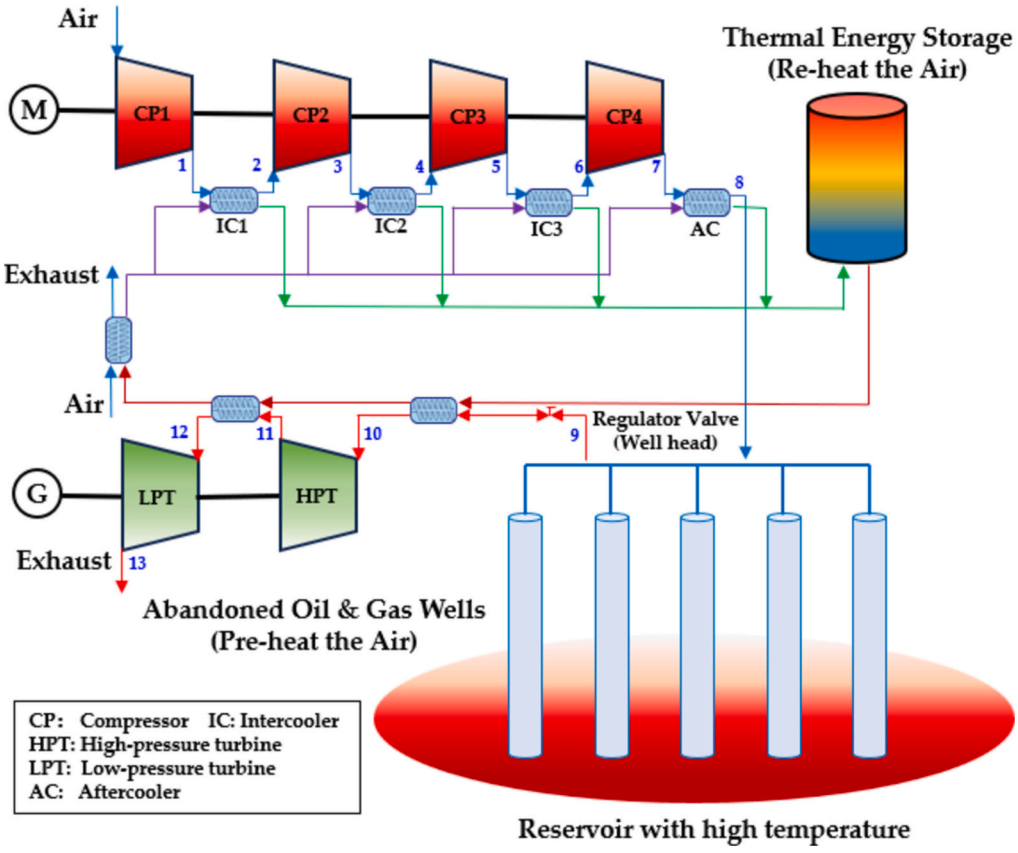

Fig. 3. Conceptual design of GA-CAES with AOGWs.

will be shut-in, awaiting a high-demand period. The hot in-situ environment at the bottomhole pre-heats the well and further pressurizes the air. (3) During high electricity demand, the air in the well is released and used to drive the turbine for electricity generation.

The GA-CAES system is innately scalable as multiple wells may be linked as alternating high- and low-pressure receptors. Wells are usually drilled in groups to aid reservoir development like water flooding. One of the most common well patterns is the five-spot well pattern as shown in Fig. 5 (a). For a five-spot well pattern with water flooding, four injection wells are located at the corners for injection with a central

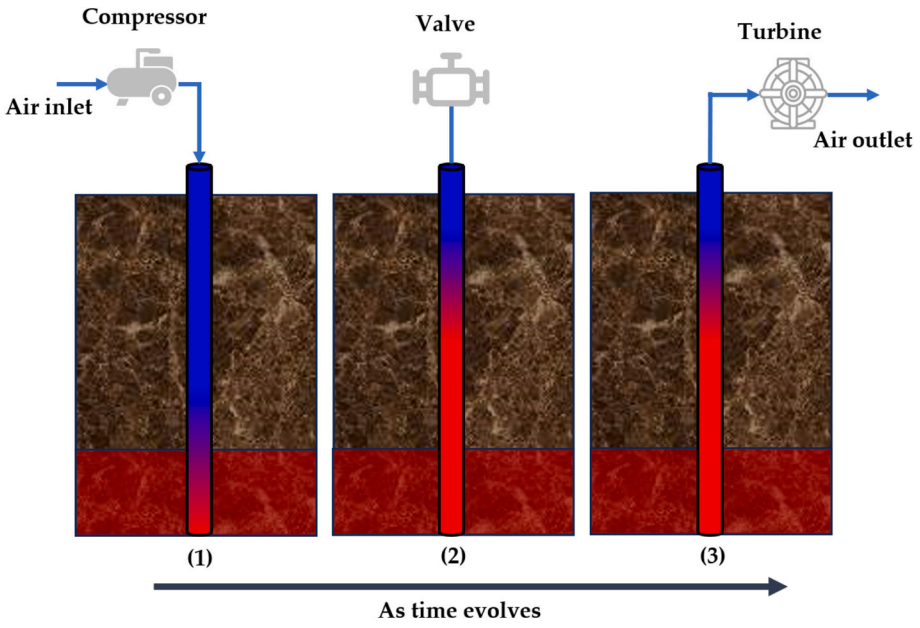

Fig. 4. A schematic of energy storage in abandoned oil and gas wells taking advantage of geothermal heat.

production well for hydrocarbon production. The injected water displaces the hydrocarbon to the production well. This is the pre-existing geometry we use to explore compressed air in AOGWs, i.e., Fig. 5 (b), which can increase the scale of energy storage for a CAES project.

The proposed GA-CAES system has several potential advantages in energy storage as follows

- Repurposing AOGWs: Leveraging existing AOGWs for renewable energy storage is an innovative approach that could significantly reduce the environmental impact of the oil and gas industry. Repurposing of AOGWs as a valuable resource provides an incentive to prevent the potential leakage of greenhouse gases
- Dual-Use Potential: We tap ubiquitous subsurface thermal energy to further increase the efficiency of the system. Utilizing AOGWs for GA-CAES while simultaneously addressing their environmental liabilities presents a compelling economic and environmental argument.
- Synergy: Integrating geothermal heat into the CAES system can enhance efficiency and further reduce reliance on external energy sources.
- Cost-Effectiveness: Reusing existing infrastructure can lead to substantial cost savings compared to constructing new facilities from scratch, and thus increase the economic efficiency of the project.

Although the proposed GA-CAES may have some advantages in future energy storage – we will quantify these advantages in the following through modeling.

This research can be divided into several parts: Regarding the air storage in the AOGWs, numerical modeling is adopted to determine the variation of pressure and temperature during the operation of GA-CAES, i.e., section 3. For all the processes on the surface, thermodynamic analysis is performed to determine the pressure and temperature throughout the system, i.e., section 4. By combining numerical modeling and thermodynamic analysis, the round-trip efficiency of the proposed GA-CAES can be evaluated. An economic analysis will follow up to determine the economic efficiency of the entire system and evaluate the feasibility of the GA-CAES in commercial applications.

3. Numerical modeling of energy storage with AOGWs

3.1. Mathematical model

We complete simulations of the full system that accommodates the transport of mass (air) and energy (heat) within the coupled system of wellbores embedded within the subsurface reservoir and linked by a surface heat exchanger.

3.1.1. Fluid flow in wellbore

It is presumed that the air in this study is the ideal gas, which adheres to the ideal gas law. The wellbore is assumed well-sealed, so we ignore any mass transfer between the wellbore and the reservoir, and we limit fluid flow to within the wellbore – independent of the reservoir. Fluid flow in the wellbore represents the transport of a single-phase (air) represented using the Navier-Stokes equation – comprising continuity and momentum balance equations for the 2D axisymmetric geometry centered on the embedded wellbore.

The continuity equation is [33].

$$\frac{\partial(\rho_f)}{\partial t}+\nabla\cdot(\rho_f\mathbf{u})=0 \tag{1}$$

where ρ_f is the fluid density. u is the vector of fluid velocity. t is the time. The normal differential operators apply.

The momentum balance equation is [33].

$$\frac{\partial(\rho_f\mathbf{u})}{\partial t}+\nabla\cdot(\rho_f\mathbf{u}\otimes\mathbf{u})=-\nabla p+\nabla\cdot\boldsymbol{\tau}+\mathbf{F} \tag{2}$$

where p is the fluid pressure. F is the tensor of the external body force. τ is the tensor of the viscous force.

The density of air inside the wellbore can be estimated as [34].

$$\rho_f=\frac{p}{ZRT} \tag{3}$$

where T is the local fluid temperature. R is the ideal gas constant. The compressibility factor Z can be expressed as [32].

$$Z=1-\frac{9p}{128p_c}\frac{T_c}{T}\left(\frac{6{T_c}^2}{T^2}-1\right) \tag{4}$$

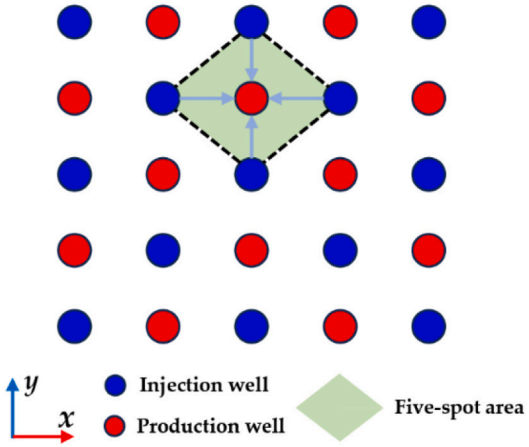

(a) Illustration of five-spot well pattern in oil and gas production.

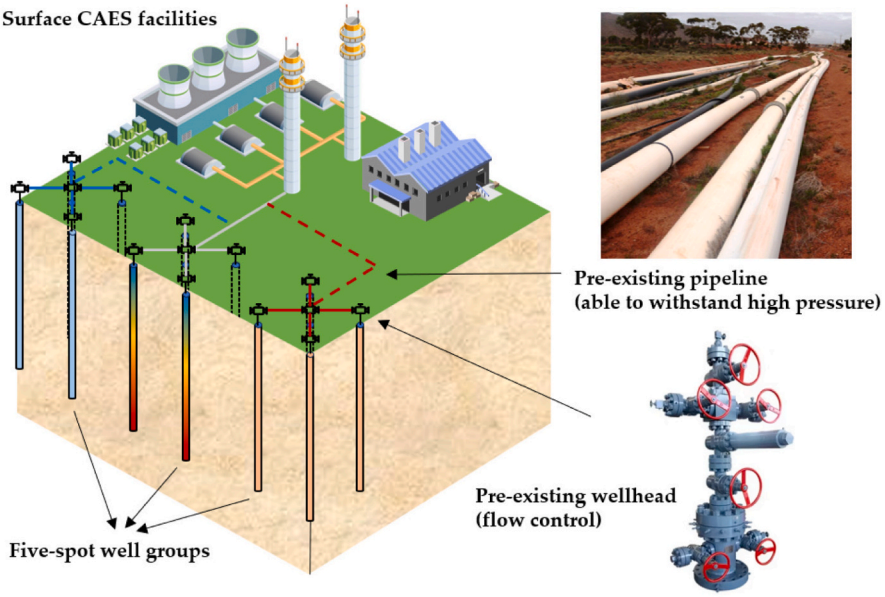

(b) Integration of abandoned well group into the GA-CAES system.

Fig. 5. A schematic of the integration of AOGWs in GA-CAES.

3.1.2. Heat transfer in AOGWs

Unlike fluid (air) flow within the wellbore, heat transfer in the GA-CAES may be divided into several components, which are: (1) Wellbore: The open space within the well; (2) Casing: The protective metal tube surrounding the wellbore; (3) Reservoir Rock: The geological formation surrounding the casing.

First, the heat transfer in the wellbore involves both heat conduction (heat transfer through a material, i.e., air, by direct contact) and heat convection (heat transfer through a fluid, i.e., in this case, the air within the wellbore). The corresponding energy balance equation can be described as [33].

$$\rho_f c_f \frac{\partial T}{\partial t} + \rho_f c_f \mathbf{u}\cdot\nabla T - \nabla\cdot(\lambda_f \nabla T) = Q_1 \tag{5}$$

where c_f is the specific heat capacity of air. λ_f is the thermal conductivity of air. Q_1 is a heat source/sink.

The assumption of a perfectly sealed wellbore implies that there is no mass transfer (e.g., fluid flow) between the wellbore and the surrounding reservoir. Then, heat transfer within the casing and reservoir rock is assumed to be purely conductive, as the materials are solid and there is no fluid flow-induced heat convection within them.

Regarding the casing, heat transfer only involves heat conduction, which can be described using Fourier's Law as [33].

$$\rho_c c_c \frac{\partial T}{\partial t} - \nabla\cdot(\lambda_c \nabla T) = Q_2 \tag{6}$$

where ρ_c is the density of the casing. c_c is the specific heat capacity of the casing. λ_c is the thermal conductivity of the casing.

Regarding the reservoir rock, since we assume that fluid within the reservoir is stagnant and can be neglected, heat transfer can also be described solely using Fourier's Law as [33].

$$\rho_s c_s \frac{\partial T}{\partial t} - \nabla\cdot(\lambda_s \nabla T) = Q_3 \tag{7}$$

where ρ_s is the density of the reservoir rock. c_s is the specific heat capacity of reservoir rock. λ_s is the thermal conductivity of rock.

Regarding the interface and boundary conditions, several equations are listed below to make connections between Eq. (5) to Eq. (7).

Wellbore-Casing Interface Ω_1: At this interface, the temperature is assumed to be continuous. This means that the temperature at the inner surface of the casing ($T_{\text{casing}}|_{\Omega 1}$) is the same as the temperature at the outer surface of the wellbore fluid ($T_{\text{wellbore}}|_{\Omega 1}$), i.e.,

$$T_{\text{wellbore}}|_{\Omega_1} = T_{casing}|_{\Omega_1} \tag{8}$$

Casing-Reservoir Rock Interface Ω_1: Similarly, the temperature is continuous at this interface. The temperature at the outer surface of the casing ($T_{\text{casing}}|_{\Omega 2}$) is equal to the temperature of the reservoir rock at the interface ($T_{\text{reservoir}}|_{\Omega 2}$).

$$T_{casing}|_{\Omega_2} = T_{\text{reservoir}}|_{\Omega_2} \tag{9}$$

The outer boundary of the reservoir Ω_3: It is assumed that the has a constant thermal gradient in the vertical direction.

$$T_{\text{reservoir}}|_{\Omega_3} = T(z) \tag{10}$$

To fully understand how these equations relate to the physical model, we also present a physical model to illustrate this process (see Fig. 6): Heat moves from the wellbore through the casing and into the reservoir rock. At the wellbore-casing interface (Ω_1) and the casing-reservoir rock interface (Ω_2), temperatures are continuous. Heat transfer within the wellbore involves both conduction and convection, while heat transfer within the casing and reservoir rock is solely through conduction. Eqs. (5), (6), and (7) describe the heat transfer within the wellbore, casing, and reservoir rock, respectively, and are coupled through the boundary conditions at the interfaces (Eqs. (8) and (9)) and outer boundary (Eq. (10)).

Based on the mathematical models presented in this section, numerical simulations can be implemented in the following sections.

3.2. Numerical implementation

In the previous section, we presented the conceptual and mathematical models for the proposed GA-CAES. Based on these mathematical models, detailed numerical implementations will be presented in this section.

For a single vertical well, the geometry can be simplified as an axisymmetric model centered around the wellbore. The physical model and computational mesh for charging and discharging a single well are shown in Figs. 7 (a) and 7 (b). The simulated reservoir has a radius of 100 m and a depth of 2000 m. We assume that the well is also drilled to 2000 m in depth, which fully penetrates the reservoir. The inner radius of the casing in this model is 0.15 m with a thickness of 2 cm. The well is cemented to 1500 m and thermal insulated material is injected into the annulus of this section to reduce the thermal influence of external

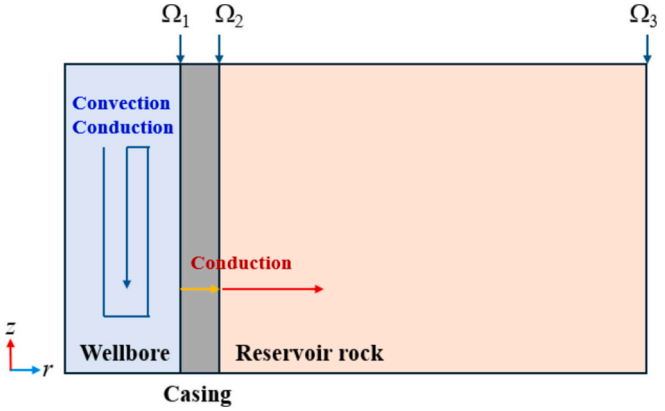

Fig. 6. Physical model of the heat transfer process in GA-CAES.

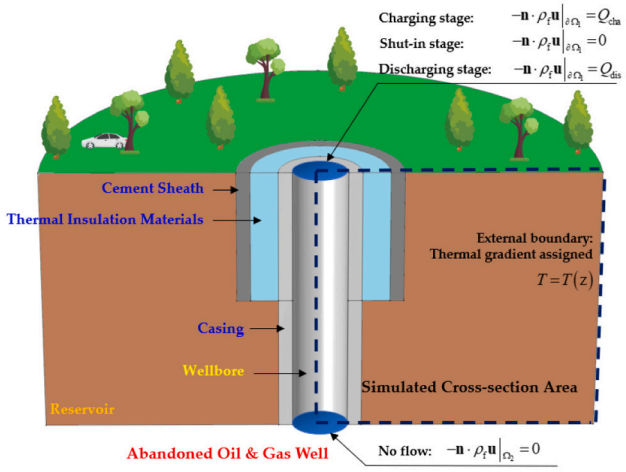

(a) Physical model for GA-CAES and simulated cross-section.

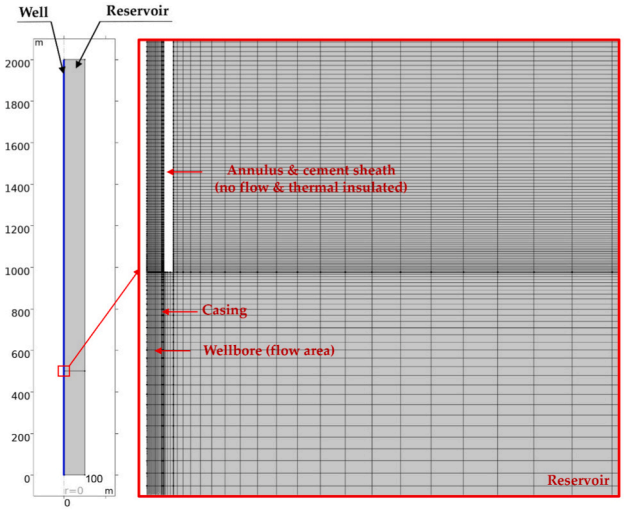

(b) Geometric model and mesh for the numerical simulation of GA-CAES.

Fig. 7. Illustration of axisymmetric model and auxiliary equations assigned in the model.

subsurface water flow at shallow depth.

An operational plan for the GA-CAES is shown in Fig. 8. For a single cycle over 24 h, the CAES operation is divided into several discrete stages. From initiation until the 12th hour, the system injects pressurized air into the wellbore at 0.25 kg/s for a single well. Then, the well is shut in for 4 h. After that, the air stored in the wellbore is discharged/produced at 0.75 kg/s for a single well from the 16th to the 20th hour. Then, the well is again shut in until the next operation cycle begins. The parameters used in the numerical simulation are listed in Table 1.

Stability and consistency of the simulation results are ensured through the correct discretization of the model in space and time and the choice of stable solution schemes. The mathematical models presented in Section 3.1 are discretized for finite element analysis (FEA). Backward differentiation (BDF) is used for the time stepping during the transient simulation with a relative tolerance for iterations of 0.01. The maximum single time step is set to 500 s to maintain stability and limit calculation errors, especially during the late calculation period.

The numerical model is validated against a reference model [35] with the simulation results from our model shown in Fig. 9. The results from the numerical solution match the reference data very well. This agreement demonstrates the suitability and accuracy of the numerical

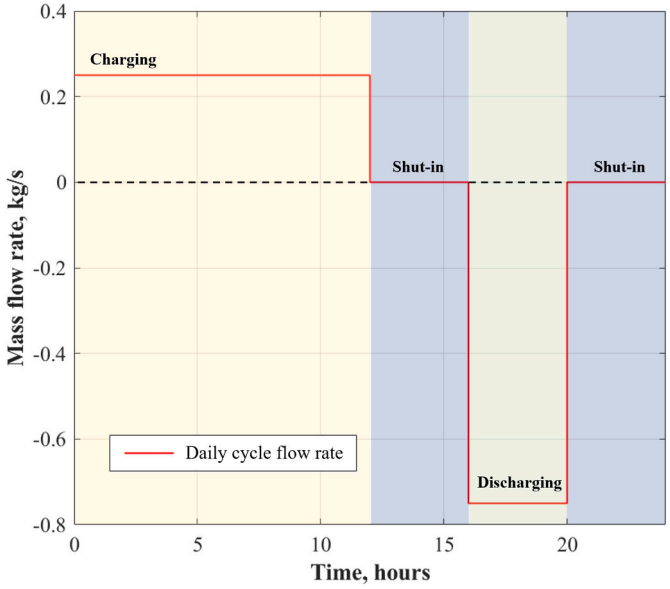

Fig. 8. Mass flow rates for a single well during a full diurnal cycle for the system.

Table 1
Parameters utilized in the numerical simulation of energy storage in a single AOGW.

Parameters	Value	Unit
Density of reservoir rock	2600	kg/m^3
Specific heat capacity of reservoir rock	980	J/(kg·K)
Thermal conductivity of reservoir rock	2.8	W/(m·K)
Density of casing	7850	kg/m^3
Specific heat capacity of casing	490	J/(kg·K)
Thermal conductivity of casing	45	W/(m·K)
The initial temperature at the wellhead	293.15	K
The initial temperature at the well bottom	473.15	K
Subsurface thermal gradient	0.09	K/m
Initial pressure at the wellhead	5.0×10^6	Pa
Simulation cycles	100	–

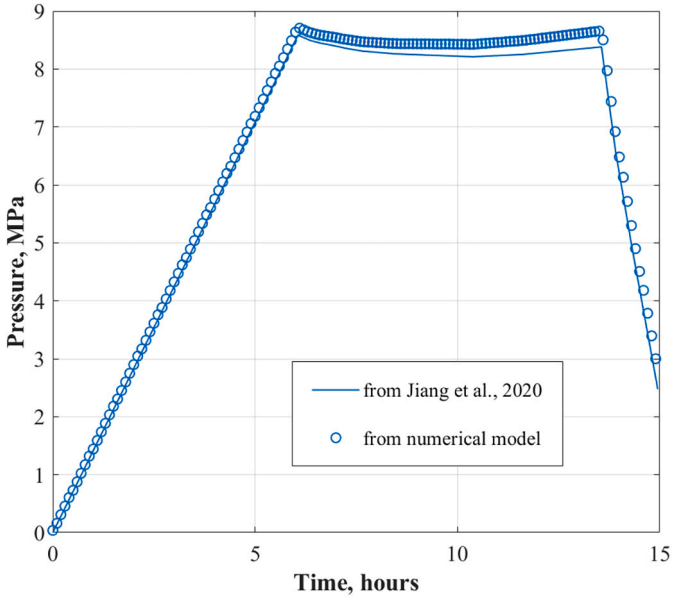

Fig. 9. Comparison between the simulation results and reference data [35].

model as a predictor for the performance of our system.

3.3. Results and discussions

In the prior section, we established a numerical model for the simulation of compressed air storage in the proposed GA-CAES. We now use this model to evaluate the performance of the proposed GA-CAES and further estimate its economic viability.

Fig. 10 shows the temperature profile in the wellbore during the first operation cycle. Initially, the air temperature in the wellbore is linearly distributed, consistent with the prescribed thermal gradient in the reservoir (see Fig. 10 (a)). Then, cold air is injected into the wellbore, significantly decreasing the temperature inside the well. The air temperature in the thermally insulated section of the well decreases towards the injection temperature (see Fig. 10 (b)). Then, the well is shut in for 4 h and during this period, hot air from the base convects upwards due to buoyancy as cold air sinks. Such a natural convection rapidly heats the wellbore, as shown in Fig. 10 (c). Subsequently, the compressed air within the wellbore is discharged to generate electricity, and the hot air from the bottom migrates to the top by forced convection (see Fig. 10 (d)). This demonstrates that geothermal heat during CAES can indeed increase the air temperature in the wellbore and preheat the air before it returns to the surface. The influence of this increase in air temperature will be discussed later.

Fig. 11 shows the temperature distribution in the wellbore and its neighborhood reservoir at the end of air injection (12th hour) in the first cycle. It can be seen from the figure that since we insulated the upper part of the wellbore (1500 m), the fluid temperature in the upper part of the wellbore can be significantly affected by the injected cold air. By contrast, for the lower part of the wellbore (500 m), the fluid temperature still remains at a high level due to the presence of external geothermal energy support. At the same time, the temperature in the surrounding reservoir rock is barely affected by the cold air injection from the wellhead. That's because only the lower part of the wellbore (500 m) has physical contact with the reservoir rock but the temperature here is always high. This display shows the feasibility of the utilization of geothermal energy and also demonstrates that this process will not contribute to any potential inter-well interference.

Fig. 12 shows the flow velocity profile in the wellbore during the first operation cycle. Initially, the air in the wellbore remains static, and the norm of fluid flow velocity in the wellbore is zero due to the equilibrium state inside the wellbore (see Fig. 12 (a)). Then, the air is injected from the wellhead for the energy storage purpose, and thus higher flow velocity can be observed. However, the flow velocity within a wellbore is not uniform (see Fig. 12 (b)). It is generally observed that the fluid velocity is higher near the center of the wellbore and lower near the wellbore wall. This phenomenon can be explained by the no-slip boundary condition applied at the wellbore wall. The no-slip boundary condition states that the fluid velocity at the solid surface (in this case, the wellbore wall) is zero. This is due to the viscous forces acting between the fluid and the solid surface. As a result, the fluid particles in direct contact with the wellbore wall are stationary (following Newton's law of viscosity). After that, as we shut-in the well again for hours, the air inside the wellbore will return to a static state again (see Fig. 12 (c)). Then, the stored air will be produced through the wellhead again (see Fig. 12 (d)). The flow velocity distribution during this time is similar to that during the air injection process (but in different directions as here we displayed the norm of velocity). However, the flow velocity during the discharging stage is much larger than that during the charging stage because the production rate at this time is much larger than the injection rate during the charging stage as shown in Fig. 8.

The evolution of depth-averaged temperature in the wellbore during 100 operation cycles is shown in Fig. 13. The system requires ~40 cycles to reach a dynamic steady state, i.e., that the maximum and minimum average air temperatures in the wellbore remain near constant with time. At the steady state, the maximum/minimum average temperatures

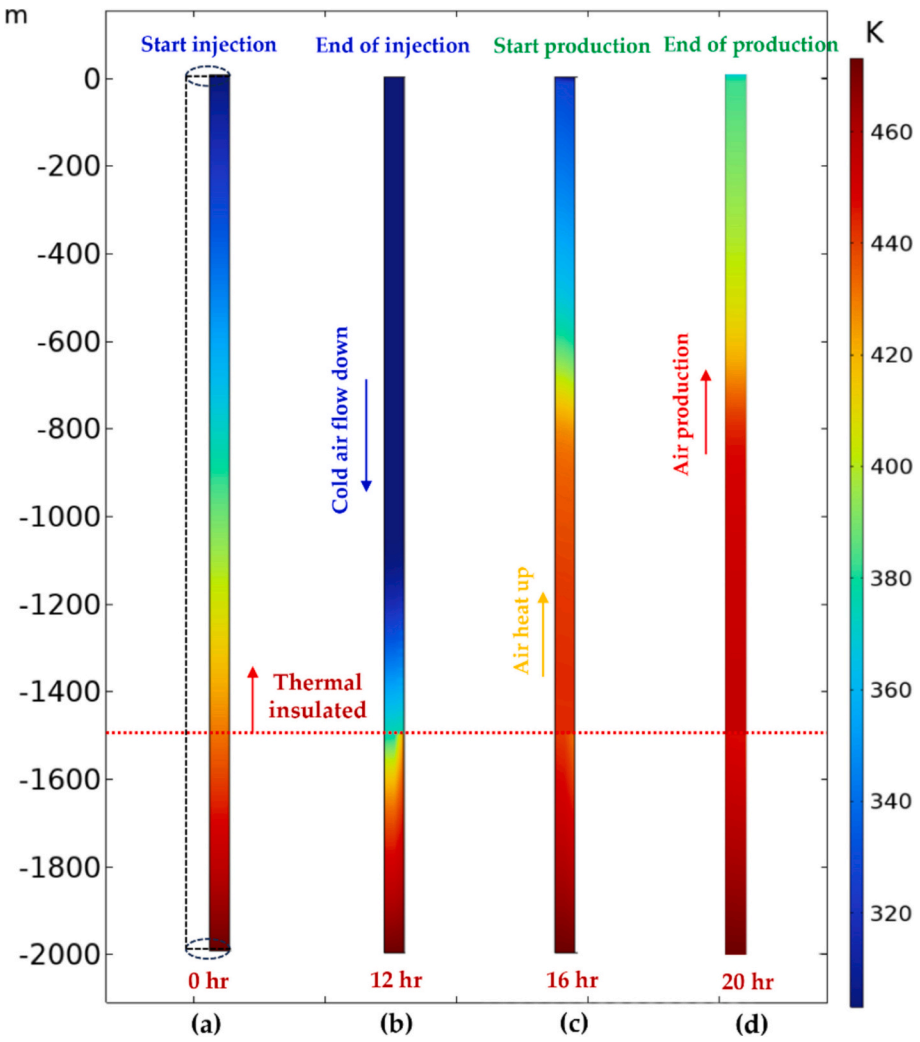

Fig. 10. Temperature distribution in the wellbore during the first operation cycle.

of air in the wellbore stabilize to 435.96/360–365 K at the end of the discharge/charge stages. The main reason for the increase in minimum average air temperature is that the air from the TES cannot be cooled down to ambient atmospheric temperature as time evolves.

An increase in average compressed air temperature in the AOGWs due to the presence of geothermal heat will also increase the air pressure. In contrast, a regular CAES system absent external heat supply will be nearly adiabatic – with pressure independent of this beneficial source of overpressure. Fig. 14 shows the variation of average air pressure in the wellbore during the first 8 cycles of GA-CAES operation both with and without geothermal heat (red line with heat and blue without). The wellbore pressure will increase from ~5 MPa to ~12 MPa – well within safe pressure constraints for typical oil and gas wells. The slight increase in pressure due to thermal effects (~0.5 MPa) will not compromise this anticipated integrity but will enhance system efficiency. The air pressure at the exit of AOGWs should be regulated to the desired pressure magnitude. For GA-CAES with AOGW, we can use the pre-existing wellhead equipment as the regulator valve. We assume that the air pressure is controlled via the Joule-Thomson throttling. Considering the narrow range of variations of the Joule-Thomoson coefficient, it is presumed that the real gas effects are neglected, and the throttling process is isothermal, i.e., the air temperature before and after traveling the valve should be the same.

4. Thermodynamic analysis

To evaluate the system efficiency of the proposed GA-CAES, we present a thermodynamic model to calculate the temperature and pressure at each step through the system. We assume an isentropic efficiency of the compressor as $\eta_{ic} = 88$ %, the mechanical efficiency of the compressor as $\eta_{mc} = 99$ %, the isentropic efficiency of the turbine as $\eta_{iT} = 88$ %, and the mechanical efficiency of the turbine as $\eta_{mT} = 99$ %. The efficiency of all the heat exchangers and recuperators is 80 % [36–38].

4.1. Compressors

In this study, the compressor train in the system is divided into several stages. The air will enter the system through the compressor with pressure first and then the compressor with high pressure. All the compressors in this paper share the same thermodynamic model.

First, the compression ratio is defined as [39].

$$\beta = \frac{p^{c}{}_{out}}{p^{c}{}_{in}} \tag{11}$$

where p^{c}_{out} is the air pressure following the compression. p^{c}_{in} is the air pressure before the compression. For the first compressor, p^{c}_{in} equals the ambient pressure.

The isentropic air temperature at the outlet of the compressor $T^{c,\,isen}_{out}$ can be evaluated as [39].

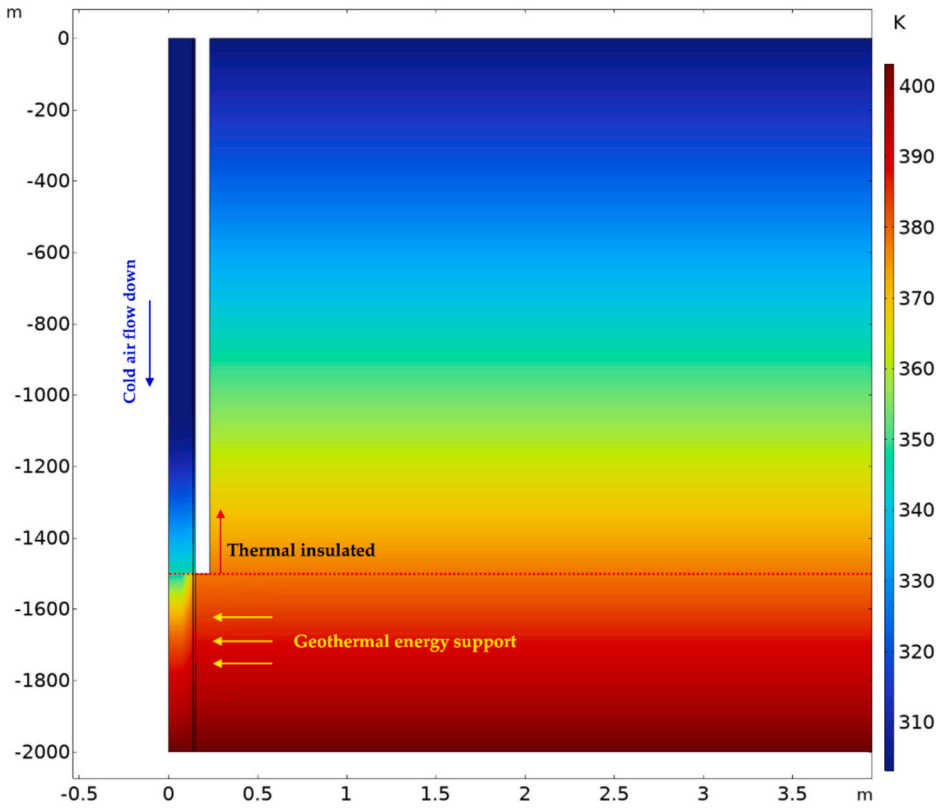

Fig. 11. Temperature distribution in the wellbore and its neighborhood reservoir at the end of air injection (12th hour) in the first cycle.

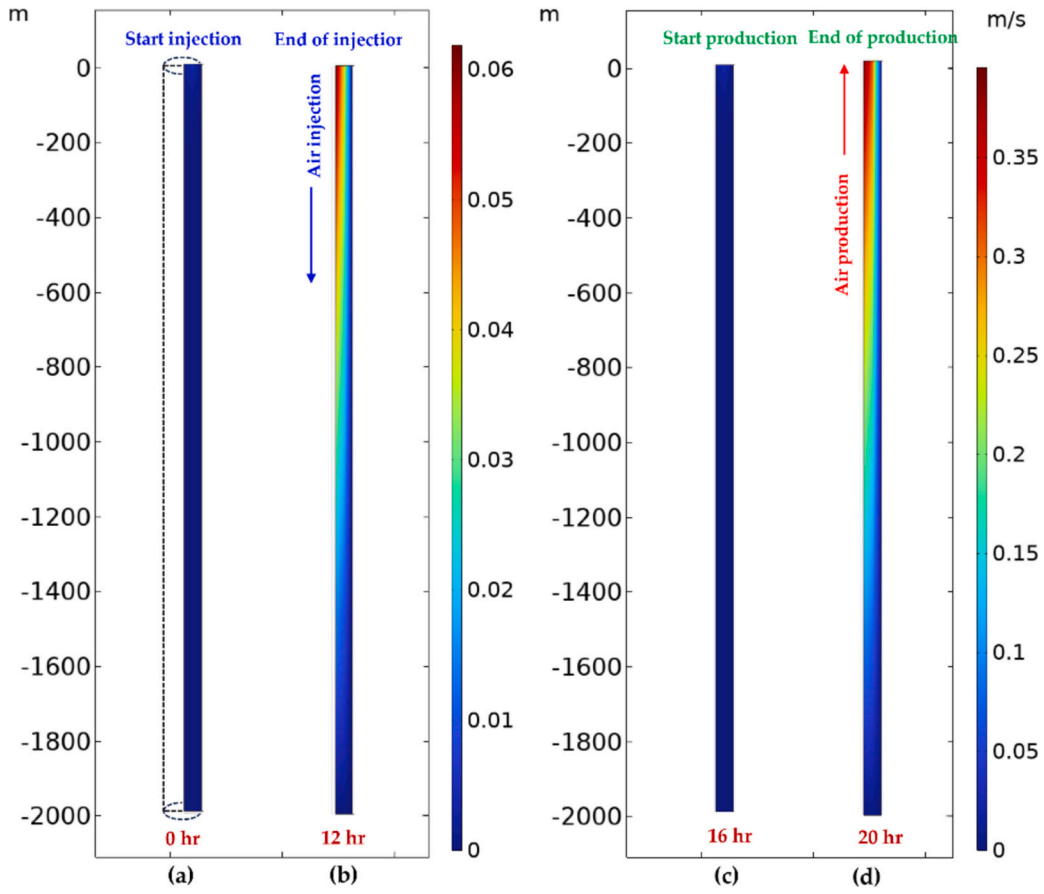

Fig. 12. Norm of velocity distribution inside the wellbore during the first operation cycle.

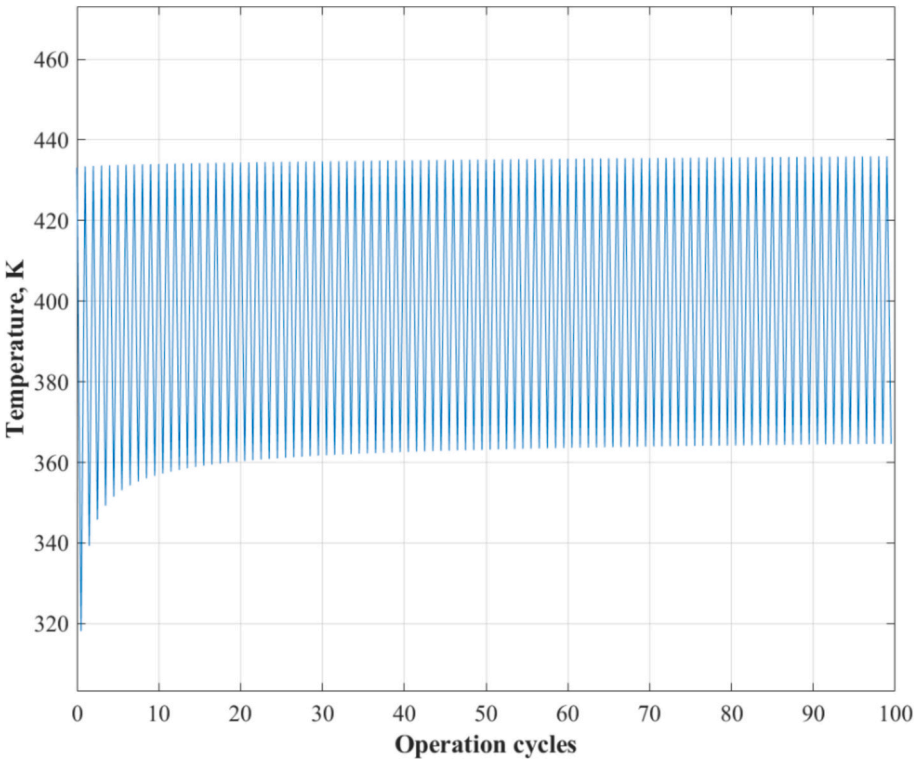

Fig. 13. Variation in the average temperature of compressed air in the wellbore over 100 operation cycles.

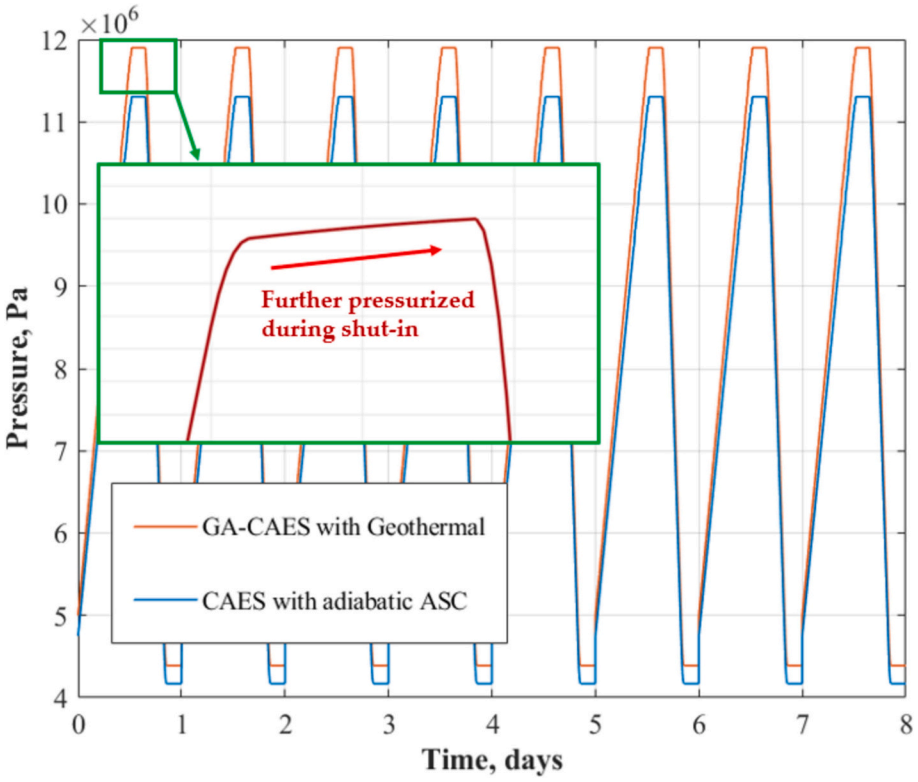

Fig. 14. Pressure variation between GA-CAES and A-CAES during the first 8 operation cycles.

$$T^{c,isen}{}_{out} = T^{c}{}_{in}(\beta)^{\frac{k-1}{k}} \tag{12}$$

where T^{c}_{in} is the air temperature at the inlet of the compressor. For the first compressor, T^{c}_{in} equals the ambient temperature. k is the specific heat ratio which is determined based on the thermodynamic property of a given working medium.

The actual air temperature at the compressor outlet can be calculated according to the definition of the isentropic efficiency of the compressor

as follows [39].

$$\eta_{ic} = \frac{T^{c,isen}{}_{out} - T^{c}{}_{in}}{T^{c}{}_{out} - T^{c}{}_{in}} \tag{13}$$

As we know the temperature at both the inlet and outlet of the compressor and mass flow rate, the power of the compressor consumed during the compression process W_c is evaluated as [39].

$$W_c = \dot{m}_c(h^{c}{}_{out} - h^{c}{}_{in}) \tag{14}$$

where h^{c}_{in} and h^{c}_{out} are the specific enthalpy at the inlet and outlet of the compressor, respectively. m_c is the mass flow rate during the compression process, equal to the injection rate in the well group.

Table 2 shows the thermodynamic calculations of the charging process for the GA-CAES.

4.2. Turbines

As noted earlier, the turbine train is divided between low-pressure turbine (LPT) and high-pressure turbine (HPT). Again, the LPT and the HPT in this paper are represented by the same thermodynamic model.

First, the expansion ratio is defined as follows [39].

$$\pi = \frac{p^{T}{}_{in}}{p^{T}{}_{out}} \tag{15}$$

where p^{T}_{out} is the air pressure after the expansion process. p^{T}_{in} is the air pressure before the expansion process.

The isentropic air temperature at the outlet of the turbine $T^{T,\,isen}_{out}$ can be calculated as [39].

$$T^{T,isen}{}_{out} = T^{T}{}_{in} \Big/ (\pi)^{\frac{k-1}{k}} \tag{16}$$

where T^{T}_{in} is the air temperature at the inlet of the turbine. k is the isentropic exponent which is determined based on the thermodynamic property of a given working medium.

The air temperature at the turbine outlet can be calculated according to the definition of the isentropic efficiency of a turbine as [39].

$$\eta_{iT} = \frac{T^{T}{}_{in} - T^{T}{}_{out}}{T^{T}{}_{in} - T^{T,isen}{}_{out}} \tag{17}$$

As we know the temperature at the inlet and outlet of the turbine and mass flow rate, the power consumed by the turbines during the discharge process W_T can be evaluated as follows [39].

$$W_T = \dot{m}_T\left(h^{T}{}_{out} - h^{T}{}_{out}\right) \tag{18}$$

where h^{T}_{in} and h^{T}_{out} are the specific enthalpy at the inlet and outlet of the compressor, respectively. m_c is the mass flow rate during the compression process, is equal to the production rate from the well group.

Table 3 shows the thermodynamic calculations for the LPT and HPT, respectively.

Table 2
Thermodynamic states during the charging process for the GA-CAES.

	T (K)	P (MPa)	C_p (kJ/kg·K)	h (kJ/kg)	β	k
0	293.15	0.1	1.006	294.91		1.4
1	455.5	0.4	1.023	465.51	4	1.391
2	350	0.4	1.01	353.5		1.399
3	542.88	1.6	1.039	564.05	4	1.383
4	450	1.6	1.025	461.25		1.392
5	679.02	6	1.071	727.2	3.75	1.367
6	550	6	1.041	572.55		1.382
7	681.99	12	1.075	733.14	2	1.366
8	313.15	12	1.007	315.3		1.4

Table 3
Thermodynamic states during the charging process for the GA-CAES.

	T (K)	P (MPa)	Cp (kJ/kg·K)	h (kJ/kg)	π	k
9	435.96	5	1.02	444.68		1.392
10	650	5	1.063	690.95		1.37
11	471.37	1.25	1.025	483.15	4	1.39
12	600	1.25	1.051	630.6		1.376
13	336.79	0.1	1.0084	339.62	12.5	1.399

4.3. Round-trip efficiency

Assuming the proposed GA-CAES system comprises 100 AOGWs, then the charging rate is 25 kg/s. Table 4 shows the input power needed for HPC and LPC based on Eq. (14).

Again, assuming the proposed GA-CAES system comprises 100 AOGWs, the charging rate is 75 kg/s. Table 5 shows the output power from HPT and LPT based on Eq. (18).

The round-trip efficiency of the system is defined as the ratio of the net total work produced in the discharge process to the net total work consumed in the charging process. Thus, the round-trip efficiency is the ratio of energy generated during the discharge process to the energy consumed during the compression process as [39].

$$\eta_{CAES} = \frac{W_T \cdot t_T}{W_c \cdot t_c} \tag{19}$$

For a GA-CAES system of 100 AOGWs, Table 6 shows the round-trip efficiency for the proposed GA-CAES and regular A-CAES. The round-trip system efficiency of the proposed GA-CAES is ~61.75 % and exceeds typical system efficiencies not augmented by geothermal heat of ~52.21 %. The comparison of round-trip efficiency between the GA-CAES and regular A-CAES indicates that the hot subsurface environment can bring identified improvement in system efficiency, which can be considered in the future CAES design.

4.3.1. Impact of downhole temperature

The system efficiency of the proposed system can be impacted by some factors. As we mentioned before, the leverage of underground geothermal energy can help to increase system efficiency. In this section, we aim to study the relationship between the downhole temperature and the round-trip efficiency.

Fig. 15 shows the change in the system efficiency according to different downhole temperatures. It can be seen that, as the downhole temperature increases, system efficiency can be increased as well. When the downhole temperature is only 313.15 K (isothermal process), the round-trip efficiency is 52.21 %, which is the same as the regular A-CAES. Then, as the reservoir temperature increases, more geothermal energy can be leveraged to pre-heat the air in the wellbore and thus the system efficiency can be increased accordingly. When the downhole temperature is 393.15 K, the system efficiency can be increased to 54.35 %. Then, as the downhole temperature increased to 473.15 K, a round-trip efficiency of 61.75 % can be expected. In general, a hotter reservoir environment can benefit the energy storage process and make the entire system operate in a much more efficient way.

4.3.2. Impact of wellbore depth

The wellbore depth determines the volume for the compressed air

Table 4
Input power needed during the charging process.

Compressors	Input Power (MW)
CP1	4.265
CP2	5.264
CP3	6.650
CP4	4.015
Total	20.19

Table 5
Output power generated during the charging process.

Turbines	Output Power (MW)
LPC	15.59
HPC	21.82
Total	37.41

Table 6
Round trip efficiency of proposed GA-CAES and regular A-CAES.

System	Round trip efficiency, %
GA-CAES	61.75
A-CAES	52.21

energy storage. A deeper wellbore can accommodate a larger charging and discharging rate. However, the depth of AOGWs in the United States varies significantly, highly depending on the age of the wellbore, and the purpose of the wellbore (conventional or unconventional). In this section, we aim to study the relationship between the wellbore depth and round-trip efficiency. In the analysis, we ensure that the average pressure in the wellbore is at the same level. In other words, deeper wellbore means larger charging and discharging rates.

Fig. 16 shows the change in the system efficiency according to different wellbore depths. It can be seen that, as the wellbore depth gets larger, system efficiency can be increased as well. When the well length is only 500 m, the round-trip efficiency is only 53.48 %. After that, as the wellbore gets deeper, more air can be pressurized and pumped into the wellbore for storage purposes and thus the system efficiency can be increased accordingly. When the well depth is 2000 m, the system efficiency can be increased to 61.75 %. Then, as the wellbore reaches 2500 m in depth, a round-trip efficiency of 65.31 % can be expected. In general, a deeper reservoir environment can benefit the energy storage process and make the entire system operate in a much more efficient way. However, this process is not perfectly linear, as deeper wellbore has higher downhole temperatures (the geothermal gradient is the same, i.e., 0.09 K/m), e.g., 338.15 K at 500 m in depth while 473.15 K at 2000 m, and thus can further increase the system efficiency.

5. Economic analysis: A case study

The profitability of the proposed GA-CAES with AOGWs can be evaluated through economic analysis. Here, the net present value (NPV) is introduced as an indicator to evaluate the economic efficiency of the system. The NPV is defined as

$$NPV_t = \sum_{t=0}^{n} \frac{R_t}{(1+i)^t} - \text{Initial investment} \tag{20}$$

where t represents time in years. n represents an incremented time step in the unit of 1 year. R_t represents the net cash flow in the t^{th} year, which is the difference between cash inflow and outflow. i is the discount rate that could be earned in alternative investments, taken as 6 % in this study.

We use the electricity price in San Franciso, CA as an example to evaluate the net cash flow in each year [40]. Table 7 shows the detailed electricity prices for different times and seasons in San Fransico.

To demonstrate the capability of CAES to maintain optimal grid stability and reliability, here we allocate different operation stages of the GA-CAES system as shown in Fig. 17. The charging stage is allocated from 10 PM to 10 AM, and the discharging stage from 2 PM to 6 AM. The intervening intervals are designated as shut-in periods for the GA-CAES system.

The operation conditions in this case study are the same as that in Sections 3 and 4. We outline some of the parameters in Table 8. Using electricity prices designated in Table 7, the GA-CAES system generates a profit of $16,237,962/year as the difference between energy generation

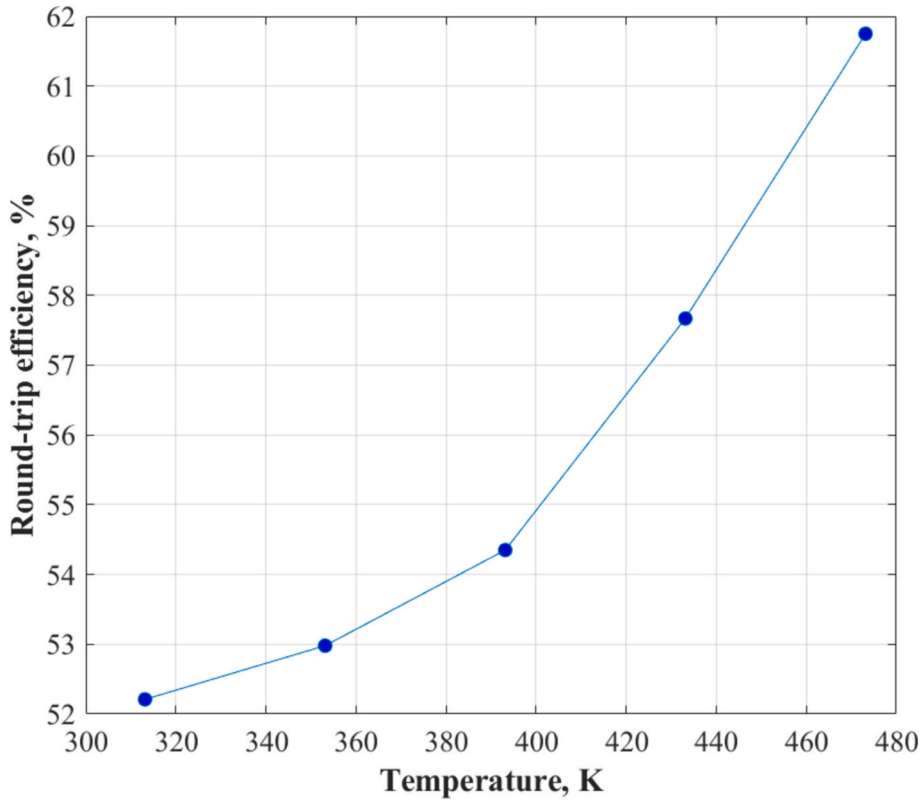

Fig. 15. The relationship between the downhole temperature and the system round-trip efficiency.

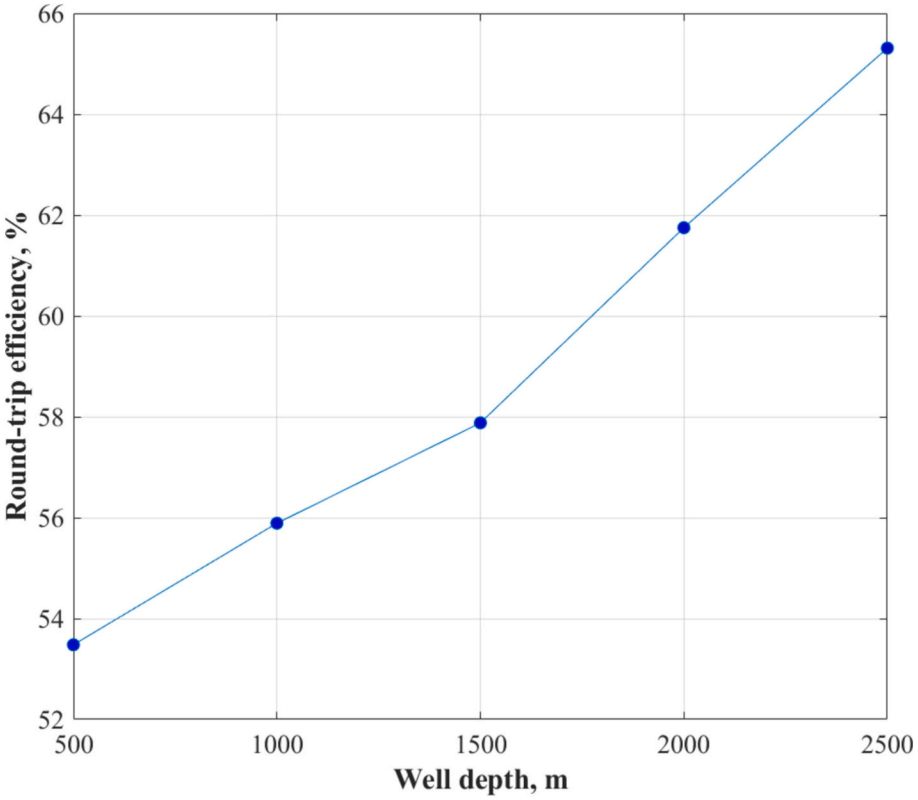

Fig. 16. The relationship between the well depth and the system round-trip efficiency.

Table 7
Electricity price (Cents/kWh) in San Francisco, CA, United States [40].

Hour	Spring	Summer	Autumn	Winter
1	2.8	3.4	2.9	3.6
2	2.3	2.9	2.5	3.1
3	1.9	2.4	2.0	2.8
4	1.7	2.2	1.8	2.6
5	1.9	2.4	2.1	2.6
6	2.4	3.1	2.6	2.8
7	2.7	3.3	3.0	2.6
8	3.1	3.7	3.4	2.9
9	3.6	5.3	3.7	3.4
10	4.2	8.0	4.2	3.9
11	4.6	17.1	5.6	4.3
12	4.8	27.3	6.4	4.6
13	5.0	39.8	8.6	4.6
14	5.6	64.4	21.4	4.7
15	7.3	83.3	34.5	5.0
16	9.3	107.5	44.8	5.2
17	8.5	98.7	45.5	5.7
18	6.5	74.8	28.7	6.0
19	5.8	37.8	15.9	5.8
20	4.9	25.6	10.8	5.7
21	5.1	41.5	10.8	6.3
22	4.7	16.1	5.6	5.1
23	4.1	6.7	4.2	4.3
24	3.4	3.1	3.6	3.7

and consumption. Fig. 18 shows the comparison of cash inflow among different seasons. The majority of the cash inflow is generated in the summer, comprising $11,293,768.92 representing ~69.55 % of the profit over the entire year. Subsequent seasons contribute 27.49 % in autumn ($4,463,879.5), 0.252 % in winter ($40,941.78), and 2.705 % in spring ($439,372.53) – the latter two represent inconsequential contributions but neither are net losses. The reason for this pattern is that, in California, summer and autumn are hot so the peak electricity price is high, allowing the generation of a significant profit. By contrast, the winter and spring in California are temperate and the difference in electricity prices cannot support significant profits. Thus, plant maintenance may be arranged for winter and spring when demand is low and the intermittency of renewables and the demand for peaking is diminished. However, different locations may yield different patterns of demand and profit. Here, we just use this case study to show how the proposed GA-CAES can contribute to regional energy supply and return of capital.

In addition to cash inflow, we also need to consider cash outflows for any project. The well drilling, sealing, and maintenance are a large part of the initial investment if AOGWs cannot be used in the proposed system. For a typical onshore oil & gas well in the United States, the well drilling cost can be described as a function of well depth according to the American Petroleum Institute (API) [42,43].

$$Z_{\text{drill}} = \left(-3.9\times10^{-8}d^3+4.0\times10^{-4}d^2-0.84d+903\right)d \tag{21}$$

where d is the well depth in m and Z_{drill} is the corresponding drilling cost. Assuming the well depth is 2000 m, the drilling cost is $1,022,000 per well. The application of AOGWs can save this part of the initial investment. Regarding the sealing, monitoring, and maintenance of the AOGWs for energy storage applications, its cost highly depends on the condition of those abandoned wells and the actual cost is unpredictable. These costs can vary widely depending on well integrity, well depth, complexity, and geological conditions. Deep wells and those with multiple completions are generally more expensive to plug. For a typical repurposed hydrocarbon field [2], the reconditioning fee (sealing and monitoring) for the abandoned wells can be up to $15,000,000 but it is still worth it, considering the cost saved including new plant site development (~$5,800,000), well site development (~$670,000), and Piping to the central facility (~$7,200,000). However, no matter how these wells will be repurposed, the sealing, monitoring, and maintenance of AOGWs can be covered by the government's funding including

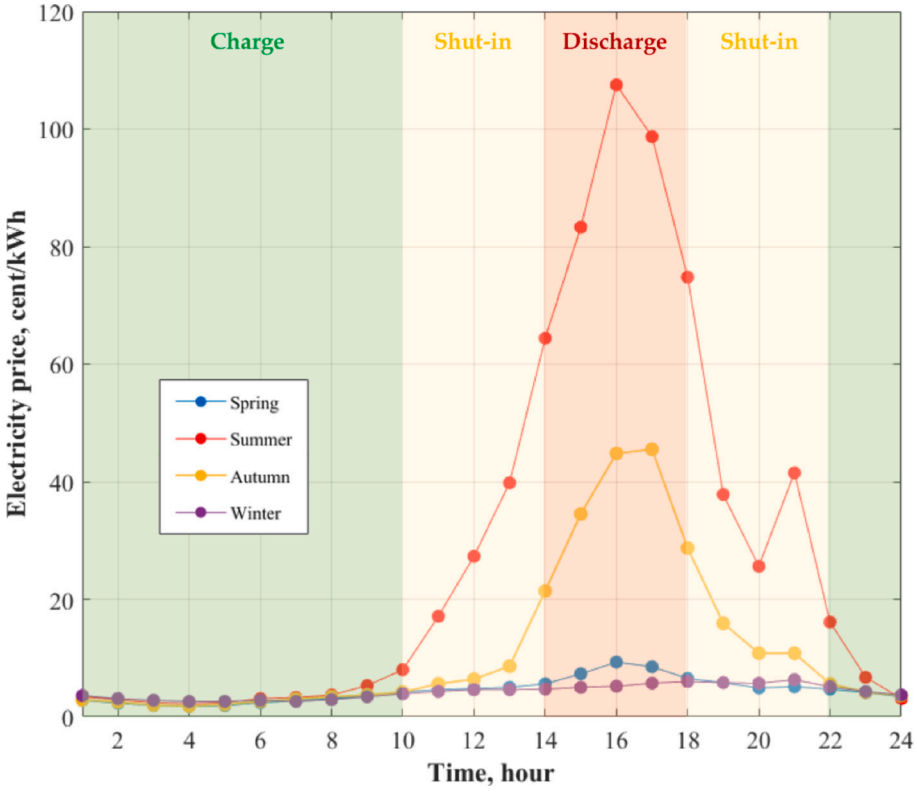

Fig. 17. Allocation of different operation stages of GA-CAES over a single day in San Francisco.

Table 8
Parameters of operation conditions utilized in the case study.

Parameters	Value	Unit
Well number	100	–
Well depth	2000	m
Total charging rate for 100 wells	25	kg/s
Total discharging rate for 100 wells	75	kg/s
The initial temperature at the wellhead	293.15	K
The initial temperature at the well bottom	473.15	K
Injected air temperature	293.15	K
Initial pressure at the wellhead	5.0×10^6	Pa

from EPA, IIJA, and state-level funding programs. By leveraging these funding sources, governments can incentivize the repurposing of AOGWs for renewable energy storage while ensuring the environmental integrity of these sites. Therefore, here we neglect this part in our estimation for both cases. The initial investment of other components in the GA-CAES can be calculated using the relationships shown in Table 9.

Fig. 19 compares the evolution of profits for the proposed GA-CAES versus a regular A-CAES. The payback period for the proposed GA-CAES is between 2 and 3 years. By contrast, the payback period of the A-CAES is between 3 and 4 years. The reason for the accelerated payback period for GA-CAES is that it leverages the use of pre-existing AOGWs, to significantly decrease initial investment for the project. This cost-saving is further aided by the added efficiency and productivity derived from geothermally preheating the air in the wellbore. In addition, abundant funding available for plugging AOGWs could be beneficially and plausibly re-programmed to GA-CAES conversions with beneficial outcomes for society in reducing greenhouse gas emissions, providing workforce engagement, and in maximizing grid efficiency and the adoption of renewables.

Compared to the conventional CAES, the presented GA-CAES can increase profitability in several ways. First, for conventional CAES, it is necessary to build new air storage containers and regulating valves while GA-CAES can leverage the preexisting AOGWs and wellhead equipment. Then, conventional CAES cannot use the heat captured in the compression process and need fossil fuel combustion to heat up the air during the discharging, while the GA-CAES can use the stored heat and can also use the geothermal energy in the subsurface. After that, the presented GA-CAES has the potential to be used for the abandoned wells to seal, monitor, and maintain the AOGWs in the project, while regular CAES need separate funding or investment. In conclusion, compared to conventional CAES, the proposed GA-CAES has more potential to be commercially successful.

6. Conclusions

We propose and then explore the performance of a geothermal-assisted adiabatic compressed air energy storage (GA-CAES) that integrates abandoned oil and gas wells into a renewable energy operation. Repurposing these preexisting facilities can decrease initial investment in any project and improve economic viability. The system also leverages the use of geothermal energy from the surrounding reservoir, further increasing system efficiency. Numerical simulations using coupled flow and energy transport models are represented by finite element methods – with the model validated against reference data.

Results show that the application of AOGWs in CAES can significantly increase the temperature of air within the system - further pressurizing the air in the well by ~0.5 MPa in a single cycle. By comparing against the case where geothermal heat does not augment the system, the round-trip efficiency is improved by ~9.5 %. Besides, according to the analysis of the system's economic efficiency. The application of AOGWs in CAES operations is shown to significantly decrease the initial investment cost of projects – by eliminating a significant infrastructure expense. Consequently, amortization can be completed up to 1 year earlier by simply using AOGWs - and the cash inflow in each year can reach over $10 million. The presented energy storage system can harness natural geothermal heat, thereby increasing system efficiency

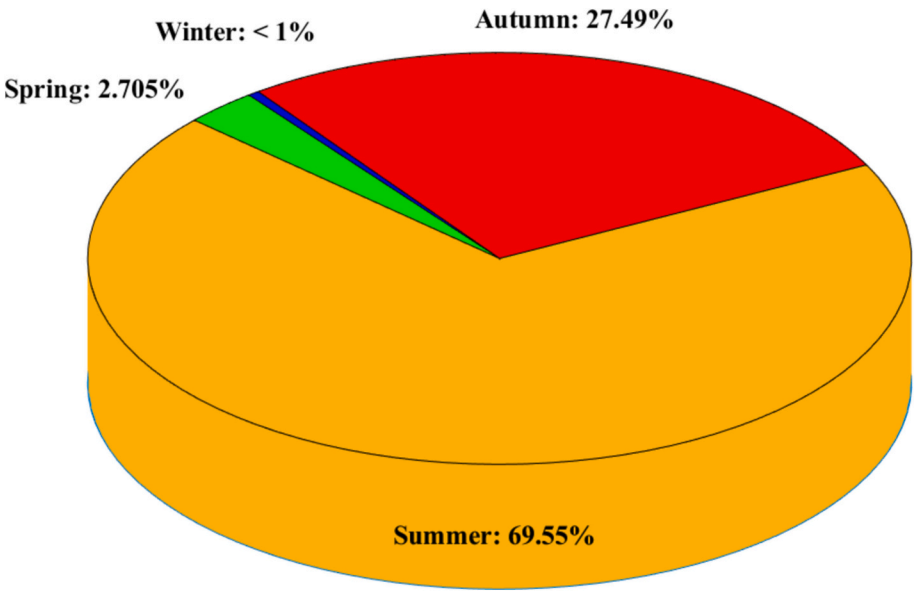

Fig. 18. Comparison of net cash inflow between different seasons within one year for San Francisco, CA.

Table 9
Capital cost formulae for each component of the CAES [41].

Components	Equation
Air compressors	$Z_{AC} = C_1 \frac{39.5\dot{m}_{in}}{0.9-\eta_{AC}} \cdot \beta \cdot ln\beta;\ C_1 = 1.051$
Air turbines	$Z_{AT} = C_1 \frac{266.3\dot{m}_{out}}{0.92-\eta_{AT}} \cdot ln\pi(1+exp(0.036T_{in}-54.4C_2));$
Pressure-regulating valves	$Z_{valve} = 114.5\dot{m}_{out}$
Heat exchangers	$Z_{Rec} = 12,000\left(\frac{A_{HEX}}{100}\right)^{0.6}$

where $C_1 = 1.051$ and $C_2 = 1.207$. β is the compression ratio of the air compressor. π is the expansion ratio of the air turbines. m_{in} and m_{out} are the air mass flow rates in the compression and expansion processes, respectively. The values of m_{in} and m_{out} are usually 2–3 times larger than that in thermodynamics analysis to accommodate special conditions. T_{in} is the air temperature before flowing into the turbine. A is the heat exchange area.

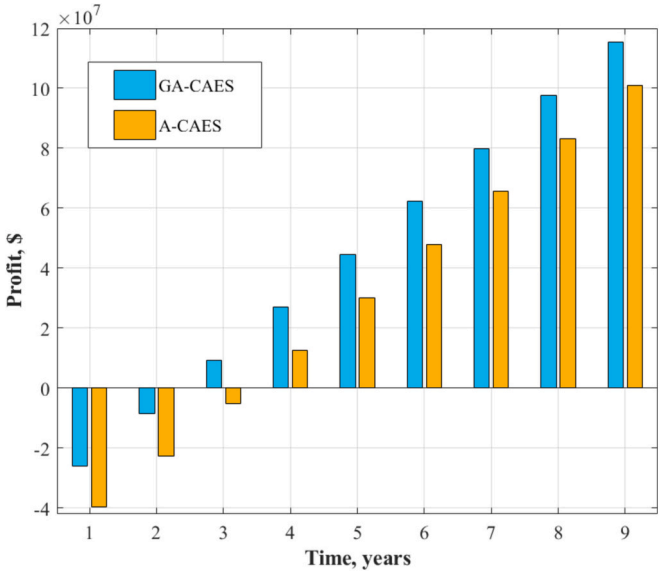

Fig. 19. The comparison of NPV and PP value between regular CAES and GA-CAES with AOGWs.

and reducing initial project costs by leveraging existing infrastructure. This study proposes then qualifies a novel method capable of boosting the efficiency of CAES and lowering the investment risk for future CAES projects – and hence elevating viability as a contributing solution to the penetration of renewables into the marketplace as a dispatchable resource.

Abbreviations

Abbreviation	Full name
A-CAES	Adiabatic compressed air energy storage
AC	Aftercooler
ADELE	Adiabatic efficient electricity storage with a LadeEinheit
AOGW	Abandoned oil and gas well
API	American Petroleum Institute
ASC	Air storage chamber
CAES	Compressed air energy storage
CP	Compressor
EPA	U.S. Environmental Protection Agency
GA-CAES	Geothermal-assisted compressed air energy storage
HPT	High-pressure turbine
IIJA	Infrastructure Investment and Jobs Act
LPT	Low-pressure turbine
NPV	Net present value
TES	Thermal energy storage

CRediT authorship contribution statement

Qitao Zhang: Writing – original draft, Investigation, Formal analysis, Data curation. **Arash Dahi Taleghani:** Writing – review & editing, Project administration, Funding acquisition, Conceptualization. **Derek Elsworth:** Writing – review & editing.

Declaration of competing interest

The authors declare that they have no known competing financial interests or personal relationships that could have appeared to influence the work reported in this paper.

Acknowledgments

The authors are grateful for financial support from the U.S. Department of Energy's Office of Energy Efficiency and Renewable Energy

(EERE) under the Geothermal Technologies Office, Award Number DE-EE0009787. The authors would also like to thank the reviewers and editors for their constructive comments on the manuscript.

Data availability

Data will be made available on request.

References

[1] M. Zhang, Q. Wang, D. Zhou, H. Ding, Evaluating uncertain investment decisions in low-carbon transition toward renewable energy, Appl. Energy 240 (2019) 1049–1060, https://doi.org/10.1016/j.apenergy.2019.01.205.
[2] L. Santos, A. Dahi Taleghani, D. Elsworth, Repurposing abandoned wells for geothermal energy: current status and future prospects, Renew. Energ. 194 (2022) 1288–1302, https://doi.org/10.1016/j.renene.2022.05.138.
[3] M. Rahman, A. Oni, E. Gemechu, A. Kumar, Assessment of energy storage technologies: A review, Energy Convers. Manag. 223 (2020) 113295, https://doi.org/10.1016/j.enconman.2020.113295.
[4] H. Ibrahim, A. Ilinca, J. Perron, Energy storage systems—Characteristics and comparisons, Renew. Sust. Energ. Rev. 12 (5) (2007) 1221–1250, https://doi.org/10.1016/j.rser.2007.01.023.
[5] S. Amrouche, D. Rekioua, T. Rekioua, S. Bacha, Overview of energy storage in renewable energy systems, Int. J. Hydrogen Energ. 41 (25) (2016) 20914–20927, https://doi.org/10.1016/j.ijhydene.2016.06.243.
[6] J. Wang, K. Lu, L. Ma, J. Wang, M. Dooner, S. Miao, et al., Overview of compressed air energy storage and technology development, Energies 10 (7) (2017) 991, https://doi.org/10.3390/en10070991.
[7] V. Tola, V. Meloni, F. Spadaccini, G. Cau, Performance assessment of adiabatic compressed air energy storage (A-CAES) power plants integrated with packed-bed thermocline storage systems, Energy Convers. Manag. 151 (2017) 343–356, https://doi.org/10.1016/j.enconman.2017.08.051.
[8] F. Crotogino, U. Mohmeyer, R. Srcharf, Huntorf CAES: More than 20 Years of Successful Operation, Orlando, Florida, USA, 2001.
[9] M. Nakhamkin, L. Andersson, E. Swensen, J. Howard, R. Meyer, R. Schainker, et al., AEC 110 Mw CAES Plant; Status of Project, in: In Proceedings of the American Power Conference, United States, 1991.
[10] C. Matos, R. Silva, F. Carneiro, Overview of compressed air energy storage projects and regulatory framework for energy storage, J. Energy Storage 55 (2022) 105862, https://doi.org/10.1016/j.est.2022.105862.
[11] H. Guo, H. Kang, Y. Xu, M. Zhao, Y. Zhu, H. Zhang, Review of coupling methods of compressed air energy storage systems and renewable energy resources, Energies 16 (12) (2023) 4667, https://doi.org/10.3390/en16124667.
[12] R. Power, ADELE–Adiabatic Compressed Air Energy Storage for Electricity Supply, RWE Power AG, Essen/Koln, 2010, p. 141.
[13] Q. Zhou, Q. He, C. Lu, D. Du, Techno-economic analysis of advanced adiabatic compressed air energy storage system based on life cycle cost, J. Clean. Prod. 265 (2020) 121768, https://doi.org/10.1016/j.jclepro.2020.121768.
[14] F. Wu, Y. Liu, R. Gao, Challenges and opportunities of energy storage technology in abandoned coal mines: a systematic review, J. Energy Storage 83 (2024) 110613.
[15] C. Matos, J. Carneiro, P. Silva, Overview of large-scale underground energy storage technologies for integration of renewable energies and criteria for reservoir identification, J. Energy Storage 21 (2019) 241–258.
[16] J. Fan, H. Xie, J. Chen, D. Jiang, C. Li, W. Tiedeu, et al., Preliminary feasibility analysis of a hybrid pumped-hydro energy storage system using abandoned coal mine goafs, Appl. Energy 258 (2020) 114007.
[17] E. Colas, E. Klopries, D. Tian, M. Kroll, M. Selzner, C. Bruecker, et al., Overview of converting abandoned coal mines to underground pumped storage systems: Focus on the underground reservoir, J. Energy Storage 73 (2023) 109153.
[18] J. Fan, W. Liu, D. Jiang, J. Chen, W. Tiedeu, J. Chen, et al., Thermodynamic and applicability analysis of a hybrid CAES system using abandoned coal mine in China, Energy 157 (2018) 31–44.
[19] C. Qin, E. Loth, Isothermal compressed wind energy storage using abandoned oil/gas wells or coal mines, Appl. Energy 292 (2021) 116867.
[20] G. Tiago Filho, G. Vela, L. da Silva, M. Perazzini, E. dos Santos, D. Fébba, Analysis and feasibility of a compressed air energy storage system (CAES) enriched with ethanol, Energy Convers. Manag. 243 (2021) 114371.
[21] J. Chen, W. Liu, D. Jiang, J. Zhang, S. Ren, L. Li, et al., Preliminary investigation on the feasibility of a clean CAES system coupled with wind and solar energy in China, Energy 127 (2017) 462–478.
[22] J. Boutot, A. Peltz, R. McVay, M. Kang, Documented orphaned oil and gas Wells across the United States, Environ. Sci. Technol. 56 (20) (2022) 14228–14236, https://doi.org/10.1021/acs.est.2c03268.
[23] U.S. Environmental Protection Agency, 2018, Access through: https://www.epa.gov/sites/default/files/2018-04/documents/ghgemissions_abandoned_wells.pdf.
[24] J. Williams, A. Regehr, M. Kang, Methane emissions from abandoned oil and gas wells in Canada and the United States, Environ. Sci. Technol. 55 (1) (2020) 563–570, https://doi.org/10.1021/acs.est.0c04265.
[25] R. Thiessen, G. Achari, Abandoned oil and gas well site environmental risk estimation, Toxicol. Environ. Chem. 99 (7–8) (2017) 1170–1192, https://doi.org/10.1080/02772248.2016.1260132.
[26] M. Harleman, J. Weber, D. Berkowitz, Environmental hazards and local investment: a half-century of evidence from abandoned oil and gas wells, Assoc. Environ. Resour. Econ. 9 (4) (2022) 721–753, https://doi.org/10.7910/DVN/3OBVQL.
[27] Report of U.S. Department of the Interior, 2022, Access through: https://www.doi.gov/pressreleases/through-president-bidens-bipartisan-infrastructure-law-24-states-set-begin-plugging.
[28] Infrastructure Investment and Jobs Act, 2022, Access through: https://www.congress.gov/bill/117th-congress/house-bill/3684?q=%7B%22search%22%3A%5B%22Transformation+to+Competitive+Employment+Act%22%5D%7D&s=1&r=1.
[29] Report of U.S. Department of the Interior, 2022, Access through: https://www.doi.gov/federal-orphaned-wells-program.
[30] S. Liu S, A. Dahi Taleghani, K. Ji, An advanced closed-loop geothermal system to substantially enhance heat production, Energ, Convers. Manag. 322 (2024) 119168, https://doi.org/10.1016/j.enconman.2024.119168.
[31] Y. Li, Y. Liu, B. Hu, J. Dong, Numerical investigation of a novel approach to coupling compressed air energy storage in aquifers with geothermal energy, Appl. Energy 279 (2020) 115781, https://doi.org/10.1016/j.apenergy.2020.11578.
[32] J. Menéndez, J. Fernández-Oro, M. Galdo, L. Álvarez, A. Bernardo-Sánchez, Numerical investigation of underground reservoirs in compressed air energy storage systems considering different operating conditions: influence of thermodynamic performance on the energy balance and round-trip efficiency, J. Energy Storage 46 (2022) 103816, https://doi.org/10.1016/j.est.2021.103816.
[33] R. Bird, W. Stewart, E. Lightfoot, Transport Phenomena, 2nd edition, John Wiley & Sons, New York, 2000.
[34] D. Kondepudi, I. Prigogine, Modern Thermodynamics: From Heat Engines to Dissipative Structures, 2nd edition, John Wiley & Sons, West Sussex, 2014.
[35] Z. Jiang, P. Li, D. Tang, H. Zhao, Y. Li, Experimental and numerical investigations of small-scale lined rock cavern at shallow depth for compressed air energy storage, Rock Mech. Rock. Eng. 53 (2020) 2671–2683, https://doi.org/10.1007/s00603-019-02009-x.
[36] A. Razmi, M. Soltani, M. Torabi, Investigation of an efficient and environmentally-friendly CCHP system based on CAES, ORC and compression-absorption refrigeration cycle: energy and exergy analysis, Energy Convers. Manag. 195 (2019) 1199–1211.
[37] S. Alirahmi, S. Mousavi, A. Razmi, P. Ahmadi, A comprehensive techno-economic analysis and multi-criteria optimization of a compressed air energy storage (CAES) hybridized with solar and desalination units, Energ. Convers. Manag. 15 (2021) 236:114053.
[38] S. Mousavi, P. Ahmadi, A. Pourahmadiyan, P. Hanafizadeh, A comprehensive techno-economic assessment of a novel compressed air energy storage (CAES) integrated with geothermal and solar energy, Sustain. Energy Technol. 47 (2021) 101418.
[39] J. Menéndez, J. Fernández-Oro, M. Galdo, L. Álvarez, A. Bernardo-Sánchez, Numerical investigation of underground reservoirs in compressed air energy storage systems considering different operating conditions: influence of thermodynamic performance on the energy balance and round-trip efficiency, J Energy Storage 46 (2022) 103816.
[40] N. Nezamoddini, Y. Wang, Real-time electricity pricing for industrial customers: survey and case studies in the United States, Appl. Energy 195 (2017) 1023–1037, https://doi.org/10.1016/j.apenergy.2017.03.102.
[41] S. Mousavi, M. Adib, M. Soltani, A. Razmi, J. Nathwani, Transient thermodynamic modeling and economic analysis of an adiabatic compressed air energy storage (A-CAES) based on cascade packed bed thermal energy storage with encapsulated phase change materials, Energy Convers. Manag. 243 (2021) 114379, https://doi.org/10.1016/j.enconman.2021.114379.
[42] American Petroleum Institute, Joint Association Survey on Drilling Costs, Washington, DC, USA, 2004.
[43] J. Ogden, N. Johnson, N, Techno-economic analysis and modeling of carbon dioxide (CO2) capture and storage (CCS) technologies, in: Developments and Innovation in Carbon Dioxide (CO2) Capture and Storage Technology, Woodhead Publishing, 2010, pp. 27–63.